

# Vertical sleeve gastrectomy increases duodenal *Lactobacillus* spp. richness associated with the activation of intestinal HIF2 $\alpha$ signaling and metabolic benefits



Yikai Shao<sup>1,2</sup>, Simon S. Evers<sup>1</sup>, Jae Hoon Shin<sup>1</sup>, Sadeesh K. Ramakrishnan<sup>3</sup>, Nadejda Bozadjieva-Kramer<sup>1</sup>, Qiyuan Yao<sup>2</sup>, Yatrik M. Shah<sup>4</sup>, Darleen A. Sandoval<sup>5</sup>, Randy J. Seeley<sup>1,\*</sup>

## ABSTRACT

**Objective:** Vertical Sleeve Gastrectomy (VSG) is one of the most efficacious treatments for obesity and its comorbidities. Although a range of evidence suggests that alterations of the microbiota in the distal gut following VSG are pivotal to these metabolic improvements, the effect of surgery to alter the microbiota of the proximal intestine and its effect on host physiology remain largely unknown. As the main bacteria in the upper small intestine, *Lactobacillus* subspecies have been appreciated as important regulators of gut function. These bacteria also regulate intestinal Hypoxia- Inducible Factor 2 $\alpha$  (HIF2 $\alpha$ ) signaling that plays an integral role in gut physiology and iron absorption. In the present study, we sought to determine the impact of VSG on *Lactobacillus* spp. in the small intestine and potential downstream impacts of *Lactobacillus* spp. on HIF2 $\alpha$ , specifically in the duodenum.

**Methods:** To determine the effects of VSG on the microbiota and HIF2 $\alpha$  signaling in the duodenum, VSG surgeries were performed on diet-induced obese mice. To further probe the relationship between *Lactobacillus* spp. and HIF2 $\alpha$  signaling in the duodenum, we applied a customized high-fat but iron-deficient diet on mice to increase duodenal HIF2 $\alpha$  signaling and determined alterations of gut bacteria. To explore the causal role of *Lactobacillus* spp. in duodenal HIF2 $\alpha$  signaling activation, we chronically administered probiotics containing *Lactobacillus* spp. to high-fat-fed obese mice. Lastly, we studied the effect of lactate, the major metabolite of *Lactobacilli*, on HIF2 $\alpha$  in *ex vivo* duodenal organoids.

**Results:** There were pronounced increases in the abundance of *Lactobacillus* spp. in samples isolated from duodenal epithelium in VSG-operated mice as compared to sham-operated mice. This was accompanied by an increase in the expression of genes that are targets of HIF2 $\alpha$  in the duodenum of VSG-treated mice. Activating HIF2 $\alpha$  signaling with a high-fat but iron-deficient diet resulted in weight loss, improvements in glucose regulation, and increased *Lactobacillus* spp. richness in the duodenum as compared to mice on an iron-replete diet. Chronic administration of probiotics containing *Lactobacillus* spp. not only increased HIF2 $\alpha$  signaling in the duodenum such as occurs after VSG but also resulted in reduced weight gain and improved glucose tolerance in high-fat-fed mice. Furthermore, lactate was able to activate HIF2 $\alpha$  in *ex vivo* duodenal organoids.

**Conclusions:** These results support a model whereby VSG increases duodenal *Lactobacillus* richness and potentially stimulates intestinal HIF2 $\alpha$  signaling via increased lactate production.

© 2022 The Author(s). Published by Elsevier GmbH. This is an open access article under the CC BY-NC-ND license (<http://creativecommons.org/licenses/by-nc-nd/4.0/>).

**Keywords** Vertical sleeve gastrectomy; Gut microbiota; *Lactobacillus*; Hypoxia-inducible factor 2 $\alpha$ ; Obesity

## 1. INTRODUCTION

Vertical sleeve gastrectomy (VSG) is currently one of the most efficacious treatments for individuals with obesity [1,2]. This bariatric procedure involves excising ~80% of the stomach along the greater curvature without rerouting the flow of chyme through the intestine as occurs in bypass procedures. While this surgical approach does not

alter the anatomy of the intestinal tract, intestinal handling of nutrients and gut hormone secretion is significantly altered after VSG [3–5]. Although incompletely elucidated, many of these physiological changes have been proposed to contribute to the sustained metabolic improvements experienced by patients following VSG [4,5]. Consequently, revealing the effects that VSG has on intestinal function and communication with other organs is a key research goal that has

<sup>1</sup>Department of Surgery, University of Michigan, Ann Arbor, MI, USA <sup>2</sup>Center for Obesity and Metabolic Surgery, Huashan Hospital of Fudan University, Shanghai, China <sup>3</sup>Department of Medicine, University of Pittsburgh, Pittsburgh, PA, USA <sup>4</sup>Departments of Molecular & Integrative Physiology, University of Michigan, Ann Arbor, MI, USA <sup>5</sup>Department of Pediatrics, Section of Nutrition, University of Colorado Anschutz Medical Campus, Aurora, CO, USA

\*Corresponding author. University of Michigan, 2800 Plymouth Rd., NCRC Building 26-343N, Ann Arbor, MI 48109-2800, USA. E-mail: [seeleyrj@med.umich.edu](mailto:seeleyrj@med.umich.edu) (R.J. Seeley).

**Abbreviations:** HIF, Hypoxia-Inducible Factor; NMR, nuclear magnetic resonance; VSG, Vertical Sleeve Gastrectomy

Received November 20, 2021 • Revision received December 25, 2021 • Accepted January 1, 2022 • Available online 6 January 2022

<https://doi.org/10.1016/j.molmet.2022.101432>

implications for both understanding the role of the gut in metabolic regulation and potential therapeutic strategies that would mimic the potential beneficial effects of these surgeries but with less invasive approaches that do not require permanent alterations in anatomy.

The profound alterations in gut physiology that take place after VSG include changes to microbial communities that inhabit the gastrointestinal tract. These microbial communities have been hypothesized to play an important role in regulating a wide range of processes in the host including body weight, body fat, and glucose regulation [6–8]. This range extends to the effects of surgical procedures such as VSG. Both human and rodent studies have documented several alterations of the relative abundance of specific bacteria following VSG [9–17]. For example, VSG has been shown to partially restore the disrupted composition of gut microbiota caused by high-fat diet (HFD) feeding and the resulting weight gain [14,15]. While still controversial, some data even point to a causal role for these changes in the gut microbiota to mediate some aspects of surgical interventions. For instance, a brief perioperative exposure to antibiotics abrogates the capacity of VSG to cause weight loss [11], while the transfer of post-gastric bypass gut microbiota to germ-free mice has induced the loss of both body weight and fat [18].

The majority of such studies have focused on bacteria collected from the feces that inhabit the large bowel and cecum because in the large bowel and cecum the largest and most easily available populations of bacteria are located. However, most work that examines the impact of the gut on systemic physiology focuses on the myriad processes and signals generated in the small intestine where most nutrient and caloric absorption occurs. Consequently, it is reasonable to hypothesize that even though the abundance of bacteria is lower in the small intestine, the impact of the microbiome on physiology may be more relevant to the small intestine.

Though the upper small intestine has emerged as a critical location for metabolic regulation [19], the main bacteria that reside there (i.e., *Lactobacillus* subspecies), are also being increasingly more appreciated as important regulators of metabolic homeostasis [20–23]. *Lactobacilli*, the gram-positive bacteria, are aerotolerant anaerobes and are generally thought to be “healthy” bacteria found in a variety of foods such as yogurt. Probiotics containing various strains of *Lactobacillus* are used to treat a wide number of gut disorders and can protect the host from some pathogens [24]. *Lactobacilli* are generally homofermentative with the end product being lactate/lactic acid.

Consistent with being a healthy bacterium, *Lactobacillus* abundance is significantly reduced by high-fat feeding, while transferring the upper small intestinal microbiota from low-fat fed rats directly into the duodenum of high-fat-fed rats can restore its richness and promote metabolic improvements, suggesting a metabolically beneficial role of duodenal *Lactobacillus* [22]. Accumulating evidence points toward important antidiabetic effects of metformin being mediated in the lumen of the gut and that metformin is also associated with an increase in *Lactobacillus* [21]. The above results corroborate recent evidence that *Lactobacillus*-containing probiotics reduce obesity in both humans and rodents [25,26]. Most relevant to the current study, data gathered from several VSG studies in rodents also indicate a substantial rise of *Lactobacillus* richness in the feces or cecal contents following VSG [12,13,16,17]. Hence, dietary, pharmacological, and surgical treatments for metabolic disease all may result in increased *Lactobacillus* spp.

A number of hypotheses have been proposed to understand how gut bacteria impact the metabolic regulation of the host [8]. One possibility is that gut microbes interact with intestinal pathways that exert influence on the host's overall physiology. An interesting aspect of this

hypothesis is that while the bulk of the bacteria in the gut reside in the colon, the bacteria most relevant might be in the small intestine. One potential target for small intestine bacteria could be hypoxia-inducible factor 2 $\alpha$  (HIF2 $\alpha$ ). HIF2 $\alpha$  regulates several crucial elements for iron absorption primarily in the duodenum [27,28]. We have found that both VSG and gastric bypass result in a profound and consistent increase in HIF2 $\alpha$  signaling in the duodenum [29]. Further, HIF2 $\alpha$  is a target for the gut microbiome where *Lactobacillus* species can directly stimulate HIF2 $\alpha$  in the intestinal epithelium cells [30–32].

Using a mouse model of VSG, we found that VSG led to metabolic improvements, associated with the increased richness of *Lactobacillus* spp. and activated HIF2 $\alpha$  signaling, specifically in the duodenum. Meanwhile, diet-induced duodenal HIF2 $\alpha$  activation was also related to metabolic improvements and increased *Lactobacillus* spp. richness in the duodenum in HFD-fed obese mice. Chronic administration of probiotics that contain *Lactobacillus* spp. resulted not only in reduced weight gain and improved glucose tolerance in HFD-fed mice but also upregulated HIF2 $\alpha$  signaling in the duodenum. Further, lactate, the major metabolite of *Lactobacilli*, activated HIF in duodenal enteroids collected from HIF-luciferase reporter mice. Overall, these data indicate that VSG increases the richness of *Lactobacillus* spp. in the duodenum and this is associated with increased intestinal HIF2 $\alpha$  signaling, resulting in multiple metabolic benefits.

## 2. MATERIALS AND METHODS

### 2.1. Animal study

To determine the effects of VSG on the gut microbiota and intestinal HIF signaling, thirty 6-week-old male ‘C57 black 6’ (C57BL6/J) mice were utilized. Prior to surgery, all mice were fed a 45% HFD (#115244, custom 45% FDC AIN-93G, Dyets Inc., Bethlehem, PA, USA) for 12 weeks. Post that, the diet-induced obese mice were randomized to undergo either VSG (n = 20) or sham surgery (SHAM, n = 10) based on their weight. All the mice were maintained on the same diet for 4 weeks after surgery until euthanasia. An intraperitoneal glucose tolerance test was performed 4 weeks post-surgery. One mouse in the VSG group failed to recover from the surgery and was excluded for any given analysis.

To determine the link between diet-induced duodenal HIF2 $\alpha$  activation and the changes to the gut microbiota in the context of metabolic improvements, thirty 6-week-old male C57BL6/J mice were randomized based on their weight to be fed either regular-iron 45% HFD (#115244, custom 45% FDC AIN-93G 35ppm iron, Dyets Inc., Bethlehem, PA, USA) as control regular-iron group (n = 15) or iron-deficient 45% HFD (#115243, custom 45% FDC AIN-93G 3–5ppm iron, Dyets Inc., Bethlehem, PA, USA) as an iron-deficient group (n = 15). The quantity of each element except iron in these two types of 45% HFD was identical. All mice were kept on the HFD for 16 weeks until euthanasia and an intraperitoneal glucose tolerance test was performed after 16 weeks of high-fat feeding. One mouse in the regular-iron diet group died during high-fat feeding and hence was excluded for any given analysis.

To determine the effects of VSL#3 probiotics (consisting of eight live and lyophilized strains including *Lactobacillus acidophilus*, *Lactobacillus paracasei*, *Lactobacillus plantarum*, *Lactobacillus delbrueckii subsp. bulgaricus*, *Bifidobacterium longum*, *Bifidobacterium breve*, *Bifidobacterium infantis*, and *Streptococcus thermophilus*, Sigma-Tau Healthscience, Inc., Gaithersburg, MD, USA) on diet-induced obesity and duodenal HIF signaling, fourteen 6-week-old male C57BL6/J mice were initially fed 45% HFD (#115244, custom 45% FDC AIN-93G, Dyets Inc., Bethlehem, PA) for six weeks. Thereafter, the diet-

induced obese mice were randomized based on their weight to receive daily gavage of either VSL#3 ( $20 \times 10^9$  CFU/0.2 ml,  $n = 7$ ) or vehicle (0.2 ml,  $n = 7$ ) for 8 weeks until euthanasia. All mice were fed the same diet till the end and an intraperitoneal glucose tolerance test was performed after eight weeks of treatment. One mouse in the VSL#3 group died from gavage accidentally and was excluded for any given analysis.

The mice were individually housed under a controlled temperature of 22 °C and light/dark cycle of 12 h, with *ad libitum* access to both diet and water. Body mass and food intake were monitored every week. Body fat and lean mass composition were measured using nuclear magnetic resonance (NMR, Echo Medical Systems LLC., Houston, TX, USA). All animal studies complied with all the relevant ethical guidelines for animal research and were approved by and conducted according to the guidelines of the Institutional Animal Care and Use Committee at the University of Michigan.

## 2.2. Surgical procedure

In the VSG/sham studies, all mice were provided with a liquid diet (Osmolite 1.0 Cal, Abbott Nutrition, Lake Forest, IL) the night before surgery. VSG and sham procedures were performed as previously described [12]. Briefly, after being anesthetized with isoflurane, the mice received a midline incision in the ventral abdominal wall and their stomachs were then exposed. For VSG, the lateral 80% of the stomach was transected along the greater curvature using an Endopath ETS-FLEX 35 mm Stapler (Ethicon endo-surgery, LLC, Cincinnati, OH), leaving a sleeve-shaped gastric remnant in the cavity. For sham surgery, gentle pressure was applied across the fundal and pylorus region with nontoothed blunt forceps. The abdominal wall was finally closed in layers using continuous absorbable 5-0 Vicryl Rapide sutures. Postoperatively, mice consumed Osmolite liquid diet for 4 days. All mice also received 1 ml warm saline subcutaneously for fluid replacement on the first postoperative day and subcutaneous injections of meloxicam (0.5 mg/kg) for pain relief once a day for 3 consecutive days following surgery. HFD was resumed on day 4, and all mice were maintained on it thereafter. Body weight and food intake following surgery were measured daily for the first week and then weekly.

## 2.3. Glucose tolerance test

During glucose tolerance tests, all mice were fasted for 4 h prior to intraperitoneal injections of dextrose (2 g/kg BW). Tail vein blood glucose levels were measured using Accu Chek Glucometer (Roche Diagnostics, Indianapolis, IN) at 0, 15, 30, 45, 60, 90, and 120 min post glucose administration. Area under the curve over 120 min was calculated.

## 2.4. Tissue collection

All mice were sacrificed after 4–6 h of fasting. Duodenum, terminal ileum, and cecum all were flushed with saline to retrieve the luminal chyme samples. Thereafter, the duodenum and terminal ileum were opened longitudinally, and mucosal samples were scraped off using slides. All intestinal chyme samples and mucosal samples were then snap-frozen in liquid nitrogen and stored in the  $-80$  °C freezer for further analysis.

## 2.5. qRT-PCR gene expression

Mucosal samples of duodenum and ileum were homogenized using Trizol reagent (#15596018, Thermo Fisher Scientific, Inc, Waltham, MA). RNA was then extracted using PureLink™ RNA mini kit (#12183025, Thermo Fisher Scientific, Inc, Waltham, MA) and cDNA

was isolated using iScript cDNA synthesis kit (#1708890, BioRad, Hercules, CA). The real-time quantitative PCR was conducted using a CFX-96 Real-Time System (BioRad, Hercules, CA) with SsoAdvanced™ Universal Probes Supermix (#1725284, BioRad, Hercules, CA) and TaqMan Gene Expression Assays (#4331182, Thermo Fisher Scientific, Inc, Waltham, MA). Expression levels of target genes were normalized to the RPL32 gene and Eukaryotic elongation factor 2 (Eef2) gene. IDs of all TaqMan Gene Expression Assays are as follows: *Eef2*, Mm01171435\_gH; *Rpl32*, Mm02528467\_g1; *Dmt1*, Mm00435363\_m1; *Dcytb*, Mm01335930\_m1; *Neu3*, Mm00479379\_m1; *Hif2 $\alpha$* , Mm01236112\_m1; *Pgk1*, Mm00435617\_m1; *Hif1 $\alpha$* , Mm00468869\_m1.

## 2.6. Analysis of the gut microbiota through 16S rRNA gene sequencing

The adherent microbiota community of luminal chyme samples and mucosal samples was analyzed through 16S rRNA gene sequencing in the Microbial Systems Molecular Biology Laboratories at the University of Michigan. DNA was isolated from intestinal chyme samples and mucosal samples with Qiagen MagAttract PowerMicrobiome kit (#27500-4-EP, MO BIO Laboratories, Inc., Carlsbad, CA) using an Eppendorf EpMotion liquid handling system. The V4 region of the 16S rRNA-encoding gene was then amplified from the extracted DNA using the barcoded dual-index primers developed by Kozich et al. [33]. Subsequently, amplicons were sequenced on the Illumina MiSeq platform (San Diego, CA) and the 16S rRNA gene sequences were further analyzed using Quantitative Insights into Microbial Ecology [34]. Following alignment to the Greengenes database, sequences were assigned to operational taxonomic units (OTUs) based on 97% sequence similarity, and those with abundance  $<0.001\%$  of the total number of sequences were excluded [35]. Overall richness of the gut microbiota was estimated using the Chao1 index of alpha diversity which calculates the total number of different OTUs present in an intestinal sample [36]. Furthermore, overall diversity was estimated using the Shannon index which evaluates the abundance and richness of OTUs into a single value of evenness [37]. Taxonomic classifications of OTUs were annotated from phylum level to genus level. The overall composition of the gut microbiota was shown using weighted UniFrac distances between samples and further visualized using principal coordinates analysis (PCoA) [38]. Linear discriminant analysis (LDA) effect size (LEfSe) with default parameters was used to identify differentially enriched bacteria taxa in different groups [39].

## 2.7. Ex vivo enteroid culture and luciferase assay

The establishment of enteroid from mice was described previously [40]. Briefly, the duodenum was isolated from HIF-luciferase reporter mice (FVB.129S6Gt(ROSA)26Sor<sup>tm2(HIF1A/luc)Kael/J</sup>) [41] and flushed with cold PBS (10,010–049, Gibco, Thermo Fisher Scientific, Waltham, MA). Thereafter, the duodenum was opened and divided into 3–4 cm sections. Sections were placed in cold high glucose Dulbecco's Modified Eagle Medium (DMEM) and rocked to remove excess fecal matter. Each section was then placed in Gentle Cell Dissociation Reagent (#07174, STEM CELL Technology, Cambridge, MA) and rocked at 4 °C for 15 min. The luminal side was gently scraped to remove villi and then placed into a fresh Cell Dissociation Reagent and rocked at 4 °C for an additional 35 min. The sections were transferred to ice-cold PBS and shaken for 2 min to remove crypts and further filtered through a 70- $\mu$ m cell strainer. The crypts were resuspended into Reduced Growth Factor Matrigel (#354230, Corning, NY) and cultured in IntestiCult™ Organoid Growth Medium (#06005, STEM CELL Technology, Cambridge, MA). Media were changed every other day. Assays

were conducted at the indicated time point after lactate ( $\text{L-Lactate}$ , #L7022, Sigma—Aldrich, St Louis, MO) or other compound treatment such as dimethylxalylglycine (DMOG, Caymen Chemicals, MI) and deferroxamine (DFO, Sigma—Aldrich, St Louis, MO). Luciferase activity of cell extracts was conducted with the Dual-Luciferase Assay System (Promega Corporation, Madison, WI) according to the manufacturer's instructions and measured with SpectraMax M5 (Molecular Devices, San Jose, CA).

### 2.8. Statistics

All data were presented in terms of means  $\pm$  S.E.M. Significant differences between two groups in body weight, cumulative food intake, blood glucose levels over time during glucose tolerance tests in all three mouse studies as well as significant differences in fat and lean mass over time between VSG and SHAM mice were assessed using two-way analysis of variance (ANOVA) with post-hoc Sidak test for multiple comparisons [42]. Otherwise, simple comparisons between two groups were evaluated with a Student's t-test except for that paired t-test and Kruskal—Wallis nonparametric test with post-hoc Dunn' multiple comparisons tests were used for related statistical analyses in [Supplementary Figs. 5 and 9](#), respectively. All statistical analyses were performed using GraphPad Prism version 8.0 software (La Jolla, CA). Data were considered statistically significant when  $P < 0.05$  (2-sided significance testing).

## 3. RESULTS

### 3.1. VSG results in metabolic improvements, associated with increased *Lactobacillus* spp. richness and activated HIF2 $\alpha$ signaling specifically in the duodenum

The 45% HFD-induced obese mice were randomized to groups undergoing either VSG or sham surgery ([Figure 1A](#)). VSG mice displayed significant reductions in body weight and cumulative food intake compared to sham-operated mice ([Figure 1B—C](#)). VSG mice also resulted in lower fat mass without a loss of lean mass as compared to SHAM mice ([Figure 1D](#)). Although fasting blood glucose levels did not differ between both groups, glucose levels from 45 to 120 min during the intraperitoneal glucose tolerance test (I.P. GTT) were substantially lower in the VSG group than in the SHAM group, leading to a significant reduction in the area under the curve (AUC) of VSG-treated mice relative to sham-operated controls ([Figure 1E](#)).

To characterize the gut microbiota changes at 4 weeks following VSG surgery, samples were collected from both luminal chyme and mucosal scrapes of the duodenum and ileum, as well as from cecum chyme for the analysis of adherent bacterial communities. The microbiome in these samples was further analyzed using 16s-rRNA sequencing. Whereas richness and diversity of the microbiota in the duodenum or ileum were lower than that in the cecum, as estimated by Chao 1 and Shannon indexes, respectively, neither Chao1 nor Shannon indexes showed differences between VSG and SHAM within each gut segment ([Supplementary Figs. 1A—B](#)). The overall composition of the gut microbiota was evaluated using weighted UniFrac PCoA. The PCoA results did not reveal markedly differential clustering of samples between VSG and SHAM within each gut segment ([Supplementary Fig. 1C](#)), suggesting no alterations in the overall composition of microbiota from proximal to distal gut following VSG.

The bacterial taxa with relative abundance varying significantly between VSG-treated and sham-operated mice within each gut segment were identified using linear discriminant analysis (LDA) effect size (LEfSe). In the duodenal chyme samples, VSG microbiota was enriched for lactic acid-carrying bacteria such as *Lactobacillus* genus and

*Bifidobacterium* genus as well as other bacteria such as *Akkermansia* genus of *Verrucomicrobia* phylum and *Bacteroidales* order, while SHAM mice were enriched for some microbes under *Proteobacteria* phylum and *Actinomycetales* order. However, in the duodenal epithelial scrape samples, VSG microbiota was enriched for only *Bifidobacterium* and *Lactobacillus*, with the latter having a high LDA score of 4, while no bacteria were identified as abundant in the duodenal mucosal sample of the SHAM group ([Figure 1F](#)). In the ileum, although *Lactobacillus* was also found considerably increased in abundance in the luminal chyme samples taken from VSG mice relative to SHAM mice, its relative richness did not differ between the two groups in the mucosal samples. On the other hand, the *Clostridiaceae* family was detected as increased in abundance in both ileum chyme and mucosal samples collected from SHAM mice. Similar to what LEfSe revealed in the ileum chyme samples, VSG and SHAM microbiota were enriched for *Lactobacillus* and *Clostridiaceae* in the cecum chyme samples, respectively ([Supplementary Fig. 2](#)).

We next determined the relative expressions of *Hif2 $\alpha$*  and its target genes in the intestine of VSG-treated and sham-operated mice. As we have observed previously [29], mRNA expressions of *Hif2 $\alpha$*  and its target genes *Dmt1*, *Dcytb* and *Neu3* were all significantly increased in the duodenum of VSG mice as compared to SHAM mice ([Figure 2A](#)), suggesting activation of HIF2 $\alpha$  signaling in the duodenum following VSG. As the HIF $\alpha$  family consists of HIF2 $\alpha$  and HIF1 $\alpha$ , we also measured the relative expressions of *Hif1 $\alpha$*  and its target gene *Pgk1*. We found no changes in *Hif1 $\alpha$*  or *Pgk1* expressions in the duodenum between VSG and SHAM groups ([Supplementary Fig. 3](#)). On the contrary, no changes were noted in the mRNA levels of *Hif2 $\alpha$*  and its target genes in the ileum of VSG-treated relative to sham-operated animals ([Figure 2B](#)), suggesting no activation of HIF2 $\alpha$  signaling in the ileum following VSG. Collectively, these data demonstrate that VSG leads to metabolic improvements in HFD-induced obese mice, associated with increased *Lactobacillus* spp. richness as well as activated HIF2 $\alpha$  signaling specifically in the duodenum.

### 3.2. Diet-induced duodenal HIF2 $\alpha$ activation is associated with metabolic improvements and increased *Lactobacillus* spp. richness in the duodenum

Given the potential association of HIF2 $\alpha$  signaling and *Lactobacillus* in the duodenum following VSG, we sought to further probe the relationship between duodenal HIF2 $\alpha$  and *Lactobacillus* in the context of metabolic improvements. HIF2 $\alpha$  signaling in the duodenum is best-known for its stimulatory effect on iron transport and iron-deficient feeding has been proven to be a definitive way to stimulate duodenal HIF2 $\alpha$  signaling [27,28]. Iron deficiency is a common outcome following bariatric surgery, including VSG [43]. Therefore, we provided a customized HFD that was also deficient in iron to C57BL/6 J mice with an attempt to mimic the effect of VSG to potentiate duodenal HIF2 $\alpha$  signaling and measure multiple metabolic parameters such as body weight and glucose tolerance as well as intestinal microbial alterations.

Male adult mice were randomized to be fed either a regular-iron (35 ppm) 45% HFD or a customized iron-deficient (3—5ppm) 45% HFD ([Figure 3A](#)). The quantity of each diet element except iron in these two types of 45% HFD was identical. Following 16 weeks of diet feeding, mice on an iron-deficient diet displayed less weight gain, resulting in significantly lower body weight compared to the control group ([Figure 3B](#)). Similarly, cumulative food intake was also lower in the iron-deficient group ([Figure 3C](#)). Body composition analysis indicated considerably lower fat mass in mice fed the iron-deficient diet. To a much lesser extent, mice in the iron-deficient group displayed

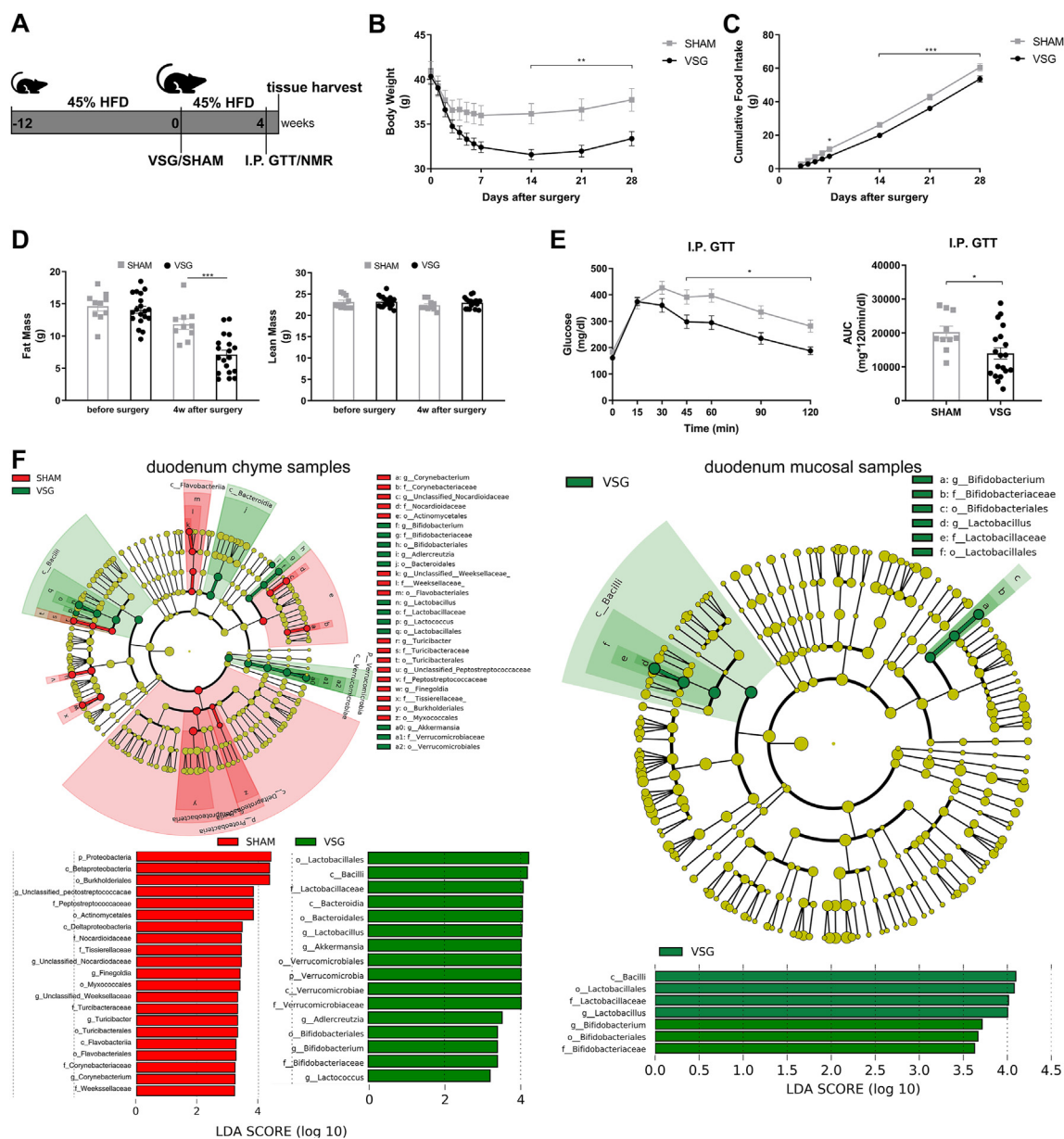


**Figure 1: VSG results in metabolic improvements in diet-induced obese mice and increases *Lactobacillus* richness in the duodenum.** **A.** Experimental design and timeline (VSG n = 19, SHAM n = 10). **B.** Bodyweight. **C.** Cumulative food intake after surgery. **D.** Fat mass and lean mass measured using nuclear magnetic resonance (NMR). **E.** Intraperitoneal glucose tolerance test (I.P. GTT, 2 g/kg) and Area Under the Curve (AUC). Data are presented as means  $\pm$  S.E.M. Two-way ANOVA with post-hoc Sidak test for multiple comparisons (Panel B–D and Panel E—I.P. GTT curve) and Student's t-test (Panel E–AUC) were used for significance assessments. \*\*\*P < 0.001, \*\*P < 0.01, \*P < 0.05. **F.** Linear discriminant analysis (LDA) effect size (LEfSe) generated phylogenetic tree and LDA score of enriched bacterial taxa in the duodenum chyme samples (left) and mucosal samples (right) collected from mice that underwent VSG and sham surgery. Significantly enriched bacterial taxa (LDA score >2 of LEfSe) were labeled with indicated colors. Abbr. SHAM, sham surgery; VSG, vertical sleeve gastrectomy.

lower lean mass as compared to the control mice (Figure 3D). Although fasting blood glucose levels were comparable between the groups, the iron-deficient group exhibited enhanced glucose tolerance as shown by lower blood glucose levels from 60 to 120 min during the I.P. GTT, resulting in a significant decline in AUC relative to the regular-iron group (Figure 3E). Together, iron-deficient feeding mice displayed marked resistance to HFD-induced weight gain and improved glucose tolerance.

To confirm the activation of intestinal HIF2 $\alpha$  signaling following iron-deficient feeding, we measured mRNA expressions of *Hif2 $\alpha$*  and its target genes in the duodenum and ileum. In the duodenum, *Hif2 $\alpha$*  and

target genes *Dmt1*, *Dcytb*, and *Neu3* were all upregulated in the deficient-iron group as compared to the regular-iron group (Figure 3F), suggesting activation of HIF2 $\alpha$  signaling in the duodenum following iron-deficient feeding. However, in the ileum, no alterations were observed in HIF2 $\alpha$  target genes expressions between both dietary groups (Supplementary Fig. 4), suggesting selective activation of HIF2 $\alpha$  signaling in the duodenum by iron-deficient feeding. Because of these differential responses of HIF2 $\alpha$  signaling to iron-deficient feeding in the duodenum and ileum, we further compared the mRNA levels of *Hif2 $\alpha$*  and its target genes between the two gut segments within each group, respectively. Both groups of mice displayed pronounced higher

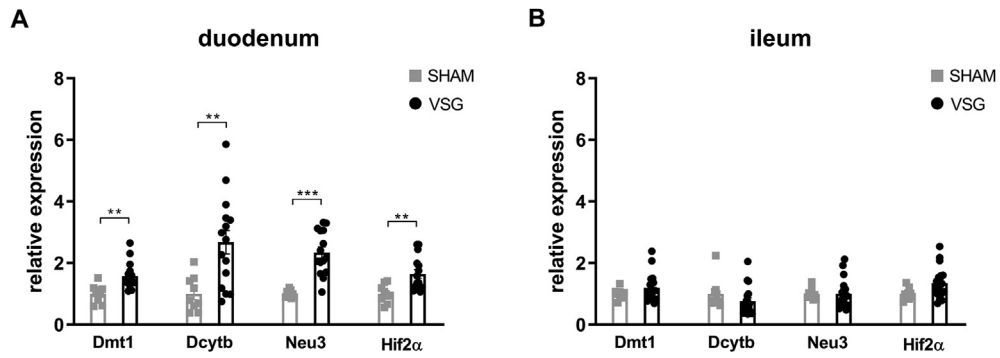


**Figure 2: VSG activates HIF2 $\alpha$  signaling in the duodenum.** Relative expressions of *Hif2 $\alpha$*  and its target genes in the **A.** duodenum and **B.** ileum of VSG-treated vs. sham-operated mice. Data are presented as means  $\pm$  S.E.M. Student's t-test was used for significance assessments. \*\*\* $P < 0.001$ , \*\* $P < 0.01$ , \* $P < 0.05$ . SHAM = sham surgery, VSG = vertical sleeve gastrectomy.

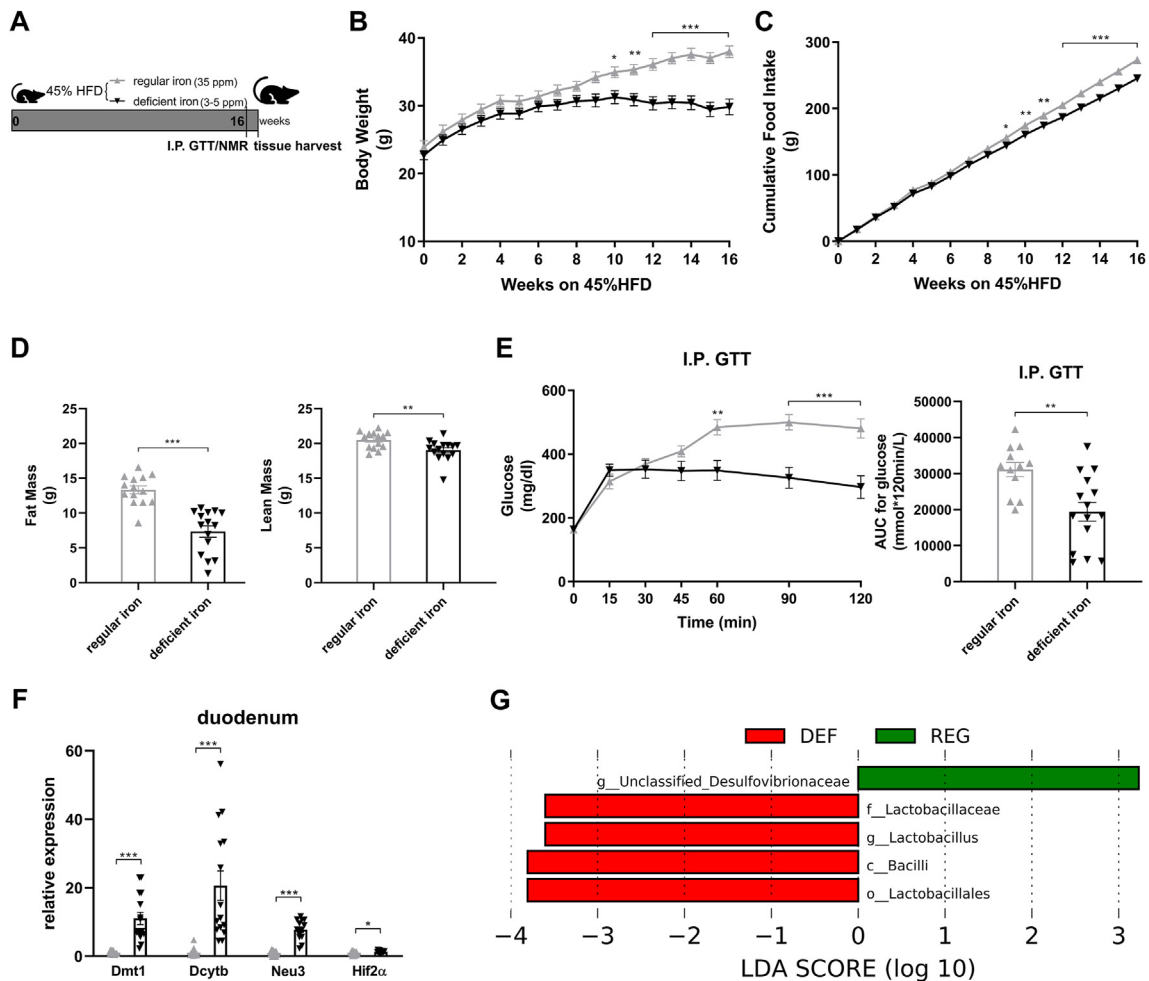


**Figure 3: Diet-induced duodenal HIF2 $\alpha$  activation is associated with metabolic improvements in high-fat-induced obese mice and increased *Lactobacillus* spp. richness in the duodenum.** **A.** Experimental design and timeline (regular-iron group  $n = 14$ , iron-deficient group  $n = 15$ ). The quantity of each element except iron in the two types of 45% high-fat diet is identical. **B.** Body weight. **C.** Cumulative food intake. **D.** Fat mass and lean mass measured using nuclear magnetic resonance (NMR). **E.** Intra-peritoneal glucose tolerance test (I.P. GTT, 2 g/kg) and Area Under the Curve (AUC). **F.** Relative expressions of *Hif2 $\alpha$*  and its target genes in the duodenum. Data are presented as means  $\pm$  S.E.M. Two-way ANOVA with post hoc Sidak test for multiple comparisons (Panels B, C, and E-I.P. GTT curve) and Student's t-test (Panel D, Panel E-AUC, and Panel F) were used for significance assessments. \*\*\* $P < 0.001$ , \*\* $P < 0.01$ , \* $P < 0.05$ . **G.** Linear discriminant analysis (LDA) effect size (LEfSe) generated LDA score of enriched bacterial taxa in the duodenum mucosal samples collected from mice of the regular-iron group (REG) and iron-deficient group (DEF). Significantly enriched bacterial taxa (LDA score  $> 2$  of LEfSe) were labeled with indicated colors.

expressions of *Hif2α* and its target genes in the duodenum than ileum (Supplementary Fig. 5), suggesting greater relevance of HIF2α signaling for the duodenum [29].

We next examined alterations to the microbiome throughout the intestine. Both luminal and mucosal adherent bacterial communities from chyme and mucosal samples of the duodenum and ileum as well as cecum chyme samples were collected from these mice. Differentially abundant microbes in the intestinal samples between both groups of mice were identified using LEfSe of the 16s-rRNA sequencing profiles. *Lactobacillus* was identified as enriched in the duodenal mucosa as well as cecum chyme samples in mice fed the iron-deficient diet (Figure 3G, Supplementary Fig. 6). In addition, we also compared the overall richness, diversity, and composition of the gut microbiota. Few discriminative features were detected between both groups except for the cecum chyme samples where iron-deficient feeding resulted in lower estimated overall richness and diversity as well as the distinct overall composition of the gut microbiota from regular-iron feeding mice (Supplementary Fig. 7). Collectively, these data demonstrate that diet-induced duodenal HIF2α activation through

dietary iron deficiency can result in metabolic improvements in HFD-induced obese mice, which is associated with increased *Lactobacillus* spp. richness in the duodenum. The combined data suggest a strong association of duodenal HIF2α activation with *Lactobacillus* spp. enrichment in the duodenum in the context of metabolic improvements.

### 3.3. Administration of probiotics containing *Lactobacillus* spp. results in metabolic improvements and activates HIF2α signaling in the duodenum

Given that we consistently observed metabolic improvements associated with increased *Lactobacillus* richness and activated HIF2α signaling, specifically in the duodenum, we hypothesized a causal role for *Lactobacillus* to increase duodenal HIF2α signaling. To achieve this goal, we treated 45% HFD-induced obese mice with probiotics (VSL#3) containing among others various species of *Lactobacillus* spp. HFD-induced obese mice were randomized to receive daily gavage of either VSL#3 or vehicle (Figure 4A). After 8 weeks of treatment, mice receiving administration of VSL#3 had decreased body weight and

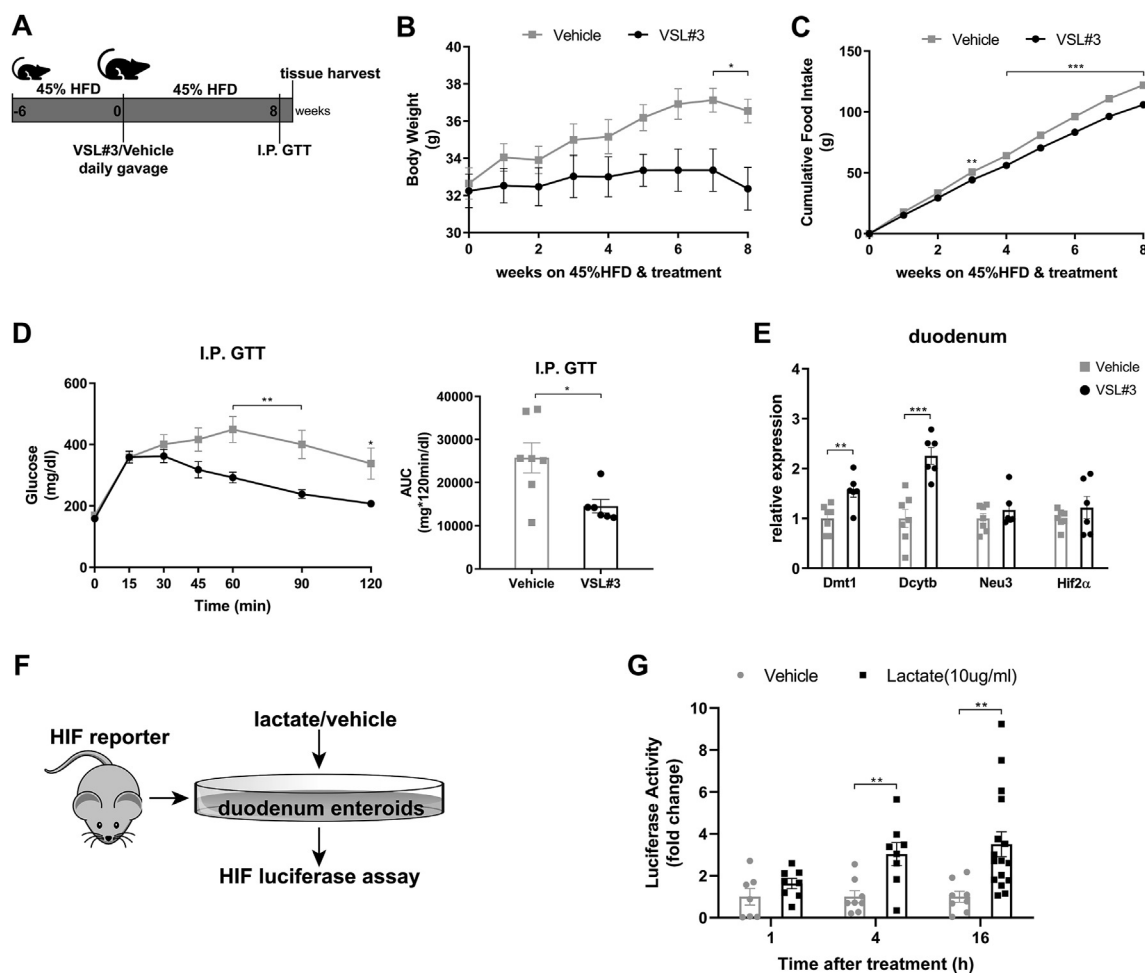


**Figure 4: Metabolic improvements and activation of HIF2α signaling in the duodenum following administration of probiotics that contain *Lactobacillus* spp. and HIF luciferase responses to lactate treatment in the organoids from HIF-reporter mice.** **A.** Experimental design and timeline of VSL#3 study (VSL#3 n = 6, Vehicle n = 7). **B.** Body weight. **C.** Cumulative food intake. **D.** Intraperitoneal glucose tolerance test (I.P. GTT, 2 g/kg) and Area Under the Curve (AUC). **E.** Relative expressions of *Hif2α* and its target genes in the duodenum of VSL#3- vs. vehicle-treated mice. **F.** Experimental design of the ex-vivo study. **G.** Luciferase activity of duodenal enteroids collected from HIF-reporter mice in response to lactate treatment (10ug/ml) vs. vehicle for indicated periods (lactate: n = 8 cell extracts for 1 and 4 h of treatment, n = 16 cell extracts for 16 h of treatment; vehicle: n = 7–8 cell extracts for each period of treatment). Data are presented as means ± S.E.M. Two-way ANOVA with post hoc Sidak test for multiple comparisons (Panel B, C, and Panel D—I.P. GTT curve) and Student's t-test (Panel D-AUC, Panel E and Panel G) were used for significance assessments. \*\*\*P < 0.001, \*\*P < 0.01, \*P < 0.05.

cumulative food intake compared to vehicle-treated mice (Figure 4B,C). During the I.P. GTT, VSL#3-treated mice exhibited better glucose tolerance relative to vehicle-treated mice, as reflected by improved glucose clearance and reduced AUC (Figure 4D). For the regulation of HIF2 $\alpha$  transcription in the duodenum, mRNA levels of Hif2 $\alpha$  and its target genes were measured. VSL#3-treated mice displayed elevated expressions of HIF2 $\alpha$  target genes such as *Dmt1* and *Dcytb* (Figure 3E), with no change in HIF1 $\alpha$  target gene *Pgk1* but substantial downregulation of *Hif1 $\alpha$*  (Supplementary Fig. 8), suggesting activation of HIF2 $\alpha$  signaling by VSL#3 in the duodenum. Taken together, administration of probiotics containing *Lactobacillus* spp. results in metabolic improvements and activates HIF2 $\alpha$  signaling in the duodenum.

### 3.4. Lactate can directly activate HIF signaling in the intestinal cells

To further evaluate the possible role of *Lactobacillus* spp. to increase duodenal HIF2 $\alpha$  signaling, we tested if lactate, a major metabolic product of *Lactobacillus*, stimulates HIF2 $\alpha$  signaling. Therefore, we examined the ability of lactate to stimulate luciferase expression in duodenal enteroids originating from HIF reporter mice [41] (Figure 3F). Initially, HIF luciferase activity was quantified following 18-hour treatment with lactate at different concentrations. Deferoxamine (DFO), dimethylxylglycine (DMOG), and hydrogen peroxide (H<sub>2</sub>O<sub>2</sub>) were used as positive controls. Lactate induced HIF reporter luciferase activity as potently as the positive controls (Supplementary Fig. 9). In view of this, HIF luciferase activity of duodenal enteroids was subsequently quantified following 1, 4, and 16 h of 10 ug/ml lactate treatment. As compared to vehicle, 4- and 16-hour lactate treatment were sufficient to elicit a respective  $3.04 \pm 0.55$  and  $3.51 \pm 0.60$ -fold rise in HIF luciferase activity (Figure 4G). Altogether, these data indicate that lactate can stimulate HIF signaling in intestinal cells, and increased *Lactobacillus*-derived lactate possibly plays a causal role in intestinal HIF activation.

## 4. DISCUSSION

A range of data point toward the gut microbiota as an important contributor to the potent metabolic improvements caused by VSG [9–15]. However, most studies concentrate on cecal or fecal microbiota. Such a focus ignores the potential contribution of bacteria residing in the proximal small intestine where many of the key events that define the GI tracts' impact on metabolism occur [19,21,22]. Towards this end, we characterized the duodenal microbiota in VSG-treated mice as compared to sham-operated control mice by sampling both luminal and mucosal adherent bacterial communities. Consistent with the extant literature [1,12], VSG resulted in metabolic improvements, accompanied by a significantly higher abundance of *Lactobacilli* in both luminal and mucosal-associated microbial communities in the duodenum. As reflected by a high LDA score of 4, *Lactobacillus* was identified as the main feature differentiating duodenal microbiota between VSG and SHAM groups (Figure 1). Interestingly, several rodent studies have revealed that at the level of the proximal small intestine, HFD feeding exerts a pronounced dysbiosis, specifically characterized by a considerable decline in the abundance of *Lactobacillus* [21,22]. In parallel, transplantation of proximal small intestinal microbiota from low-fat diet-fed rats into the duodena of HFD-fed rats has been shown to partially restore the normal abundance of *Lactobacillus* and reduce metabolic disruptions induced by HFD feeding [22]. Given the marked increase in the abundance of *Lactobacillus* in the duodenum following VSG, it is, therefore, possible that this enriched microbe contributes to the metabolic improvements imparted by VSG.

The role that the gut microbiome plays in host metabolism remains controversial partly because the mechanisms by which the microbiome can influence the host remain undefined. Herein, we hypothesize that bacterial species in the small intestine influence key signaling pathways in the intestine. HIF signaling plays an integral role in the maintenance of gut physiology and barrier integrity [27]. In particular, HIF2 $\alpha$  is a critical component of regulating iron absorption in the proximal small intestine [28]. Interestingly, we have recently found that HIF2 $\alpha$  and its target genes are upregulated in the duodenum following both VSG and gastric bypass in rodents, and activation of intestinal HIF2 $\alpha$  signaling via gut-specific knockdown of VHL results in a lean and glucose tolerant phenotype when exposed to an HFD [29]. Using a mouse model of VSG in the present study, we confirmed that VSG leads to an enhancement of HIF2 $\alpha$  signaling in the duodenum that is accompanied by an enrichment of *Lactobacillus* spp.

Other studies have shown an increased abundance of *Lactobacillus* spp. in the duodenum in connection to low iron diets that increase duodenal HIF2 $\alpha$  activation [44]. To further reveal the link between HIF2 $\alpha$  and *Lactobacillus* in the duodenum in the context of metabolic improvements as VSG induces, we applied a customized high-fat, iron-deficient diet. The iron-deficient feeding approach has been proven to significantly stimulate HIF2 $\alpha$  activities in the duodenum [28]. Consistent with previous observations [28], mice fed on an iron-deficient diet had upregulated HIF2 $\alpha$  signaling in the duodenum but not in the ileum. Importantly, these mice also recapitulated key metabolic features of VSG mice since they displayed reduced weight gain, lower fat mass, and improved glucose tolerance when challenged with high-fat feeding. Moreover, we identified that *Lactobacillus* was enriched in the duodenum mucosal samples in iron-deficient fed mice relative to control mice (Figure 3), as we found following VSG. Taken together, these data suggest a strong association between HIF2 $\alpha$  activation and *Lactobacillus* spp. enrichment in the duodenum in the context of metabolic improvements to mice maintained on an HFD.

The key question then becomes whether the increase in *Lactobacillus* is a driver of the increased HIF2 $\alpha$  signaling in the duodenum. Chronic administration of the probiotics VSL#3 in diet-induced obese mice resulted in reduced weight gain and cumulative food intake as well as improved glucose tolerance (Figure 4A–E). This is consistent with recent studies showing that VSL#3 reduces metabolic dysfunction in diet-induced obese mice [26,45]. Importantly, VSL#3 also resulted in increased HIF2 $\alpha$  signaling in the duodenum. Consequently, we hypothesized that lactate produced by *Lactobacillus* could enhance HIF2 $\alpha$  signaling. To test this hypothesis, we isolated crypts and established enteroids from the duodena of HIF-reporter luciferase mice. Treatment with lactate yielded HIF activation determined by luciferase activity, indicating that lactate can directly stimulate intestinal HIF-related signaling (Figure 4F–G). This is consistent with previous observations that multiple *Lactobacillus* spp. and strains such as *acidophilus*, *rhamnosus* GG, and *plantarum* 299v stimulate HIF2 $\alpha$  target genes expressions in intestinal epithelium cells [30–32].

The alterations to the gut microbiota following bariatric surgery are one clear example of gut adaptation to surgical manipulations on the gastrointestinal tract [3,4]. Focusing on the microbiota in the upper small intestine, we found that VSG led to the increased richness of *Lactobacillus* in the duodenum where dietary iron absorption primarily occurs. This was associated with an increase in the duodenal HIF2 $\alpha$  signaling which would work to enhance iron absorption from the lumen. Interestingly, we and others consistently found that iron-deficient diets similarly resulted in increased *Lactobacillus* richness and HIF2 $\alpha$  signaling in the duodenum [28,44], implicating a potential relationship between increased *Lactobacillus* and alterations in iron

levels in the duodenal lumen. VSG results in several changes in the lumen of the duodenum and future studies are warranted to assess the most important changes to the increased richness of *Lactobacillus*. Taken together, these results support a model whereby VSG increases duodenal *Lactobacillus* richness and this, in turn, stimulates intestinal HIF2 $\alpha$  signaling via increased lactate production. Further, activation of duodenal HIF2 $\alpha$  signaling either by diet (as done in the present study) or by genetic manipulation [29] results in multiple metabolic benefits. Understanding the molecular underpinnings for the beneficial effects of bariatric surgery remains an important research goal. These data point to the complex interplay between diet, gut bacteria, and critical aspects of gut function and signaling that combine to mediate the potent effects of bariatric surgery.

## AUTHOR CONTRIBUTIONS

Y.S., S.S.E., and R.J.S. conceived, designed experiments, and wrote the manuscript. Y.S., S.S.E., and J.S. conducted the experiments and analyzed the results. S.K.R., N.B.K., Q.Y., Y.M.S., and D.A.S. helped with data interpretation and discussion. All authors commented on and edited the manuscript. R.J.S. provided final approval of the submitted manuscript.

## ACKNOWLEDGMENTS

The authors thank the surgeons Alfor Lewis, Andriy Myronovych, Mouhamadou Toure (University of Michigan) for performing mouse VSG/sham surgeries and Kelli Rule, Jack Magrisso, and Stace Kernodle (University of Michigan) for technical assistance. We thank the Microbial Systems Molecular Biology Laboratories at the University of Michigan for microbiota sequencing. This work was supported in part by NIH grants DK117821, DK089503, DK119188 to R.J.S., NIH grants DK121995, DK107282, and American Diabetes Association grants 1-19-IBS-252 to D.A.S., NIH grants R01CA148828, R01CA245546, R01DK095201 and Center for Gastrointestinal Research DK034933 and the Department of Defense CA171086 to Y.M.S., NIH grants 5T32DK108740, 5P30DK034933, UL1TR002240 to N.B.K., China Scholarship Council grants CSC#201606100218 to Y.S., grants from National Natural Science Foundation of China 82100584 to Y.S. and 81970458 to Q.Y.

## CONFLICT OF INTEREST

R. J. S. has received research support from Novo Nordisk, AstraZeneca, and Pfizer. R. J. S. also serves as a paid consultant for Novo Nordisk, Fractyl, ShouTi Pharma and Scobia Pharma, Inc. and has taken equity positions in Calibrate and ReDesign Health. The other authors declare no conflicts of interest.

## APPENDIX ASUPPLEMENTARY DATA

Supplementary data to this article can be found online at <https://doi.org/10.1016/j.molmet.2022.101432>.

## REFERENCES

- [1] Schauer, P.R., Bhatt, D.L., Kirwan, J.P., Wolski, K., Aminian, A., Brethauer, S.A., et al., 2017. Bariatric surgery versus intensive medical therapy for diabetes - 5-year outcomes. *New England Journal of Medicine* 376(7):641–651.
- [2] Arterburn, D.E., Telem, D.A., Kushner, R.F., Courcoulas, A.P., 2020. Benefits and risks of bariatric surgery in adults: a review. *The Journal of the American Medical Association* 324(9):879–887.
- [3] Steenackers, N., Vanuytsel, T., Augustijns, P., Tack, J., Mertens, A., Lannoo, M., et al., 2021. Adaptations in gastrointestinal physiology after sleeve gastrectomy and Roux-en-Y gastric bypass. *The Lancet. Gastroenterology and Hepatology* 6(3):225–237.
- [4] Evers, S.S., Sandoval, D.A., Seeley, R.J., 2017. The physiology and molecular underpinnings of the effects of bariatric surgery on obesity and diabetes. *Annual Review of Physiology* 79:313–334.
- [5] Sinclair, P., Brennan, D.J., le Roux, C.W., 2018. Gut adaptation after metabolic surgery and its influences on the brain, liver and cancer. *Nature Reviews Gastroenterology & Hepatology* 15(10):606–624.
- [6] Maruvada, P., Leone, V., Kaplan, L.M., Chang, E.B., 2017. The human microbiome and obesity: moving beyond associations. *Cell Host & Microbe* 22(5):589–599.
- [7] Ridaura, V.K., Faith, J.J., Rey, F.E., Cheng, J., Duncan, A.E., Kau, A.L., et al., 2013. Gut microbiota from twins discordant for obesity modulates metabolism in mice. *Science* 341(6150):1241214.
- [8] Fan, Y., Pedersen, O., 2021. Gut microbiota in human metabolic health and disease. *Nature Reviews Microbiology* 19(1):55–71.
- [9] Liu, R., Hong, J., Xu, X., Feng, Q., Zhang, D., Gu, Y., et al., 2017. Gut microbiome and serum metabolome alterations in obesity and after weight-loss intervention. *Nature Medicine* 23(7):859–868.
- [10] Gralka, E., Luchinat, C., Tenori, L., Ernst, B., Thurnheer, M., Schultes, B., 2015. Metabolomic fingerprint of severe obesity is dynamically affected by bariatric surgery in a procedure-dependent manner. *The American Journal of Clinical Nutrition* 102(6):1313–1322.
- [11] Jahansouz, C., Staley, C., Kizy, S., Xu, H., Hertzler, A.V., Coryell, J., et al., 2019. Antibiotic-induced disruption of intestinal microbiota contributes to failure of vertical sleeve gastrectomy. *Annals of Surgery* 269(6):1092–1100.
- [12] Ryan, K.K., Tremaroli, V., Clemmensen, C., Kovatcheva-Datchary, P., Myronovych, A., Kams, R., et al., 2014. FXR is a molecular target for the effects of vertical sleeve gastrectomy. *Nature* 509(7499):183–188.
- [13] Basso, N., Soricelli, E., Castagneto-Gissey, L., Casella, G., Albanese, D., Fava, F., et al., 2016. Insulin resistance, microbiota, and fat distribution changes by a new model of vertical sleeve gastrectomy in obese rats. *Diabetes* 65(10):2990–3001.
- [14] Jahansouz, C., Staley, C., Bernlohr, D.A., Sadowsky, M.J., Khoruts, A., Ikramuddin, S., 2017. Sleeve gastrectomy drives persistent shifts in the gut microbiome. *Surgery for Obesity and Related Diseases* 13(6):916–924.
- [15] Shao, Y., Shen, Q., Hua, R., Evers, S.S., He, K., Yao, Q., 2018. Effects of sleeve gastrectomy on the composition and diurnal oscillation of gut microbiota related to the metabolic improvements. *Surgery for Obesity and Related Diseases* 14(6):731–739.
- [16] Ding, L., Zhang, E., Yang, Q., Jin, L., Sousa, K.M., Dong, B., et al., 2021. Vertical sleeve gastrectomy confers metabolic improvements by reducing intestinal bile acids and lipid absorption in mice. *Proceedings of the National Academy of Sciences of the United States of America* 118(6):e2019388118.
- [17] Bozadjieva-Kramer, N., Shin, J.H., Shao, Y., Gutierrez-Aguilar, R., Li, Z., Heppner, K.M., et al., 2021. Intestinal-derived FGF15 protects against deleterious effects of vertical sleeve gastrectomy in mice. *Nature Communications* 12(1):4768.
- [18] Liou, A.P., Paziuk, M., Luevano Jr., J.M., Machineni, S., Turnbaugh, P.J., Kaplan, L.M., 2013. Conserved shifts in the gut microbiota due to gastric bypass reduce host weight and adiposity. *Science Translational Medicine* 5(178):178ra41.
- [19] Duca, F.A., Bauer, P.V., Hamr, S.C., Lam, T.K., 2015. Glucoregulatory relevance of small intestinal nutrient sensing in physiology, bariatric surgery, and pharmacology. *Cell Metabolism* 22(3):367–380.
- [20] Donaldson, G.P., Lee, S.M., Mazmanian, S.K., 2016. Gut biogeography of the bacterial microbiota. *Nature Reviews Microbiology* 14(1):20–32.
- [21] Bauer, P.V., Duca, F.A., Waise, T., Rasmussen, B.A., Abraham, M.A., Dranse, H.J., et al., 2018. Metformin alters upper small intestinal microbiota

- that impact a glucose-SGLT1-sensing glucoregulatory pathway. *Cell Metabolism* 27(1):101–117 e5.
- [22] Bauer, P.V., Duca, F.A., Waise, T., Dranse, H.J., Rasmussen, B.A., Puri, A., et al., 2018. *Lactobacillus gasseri* in the upper small intestine impacts an ACSL3-dependent fatty acid-sensing pathway regulating whole-body glucose homeostasis. *Cell Metabolism* 27(3):572–587 e6.
- [23] Rodrigues, R.R., Gurung, M., Li, Z., García-Jaramillo, M., Greer, R., Gaulke, C., et al., 2021. Transkingdom interactions between *Lactobacilli* and hepatic mitochondria attenuate western diet-induced diabetes. *Nature Communications* 12(1):101.
- [24] Heeney, D.D., Gareau, M.G., Marco, M.L., 2018. Intestinal *Lactobacillus* in health and disease, a driver or just along for the ride? *Current Opinion in Biotechnology* 49:140–147.
- [25] Osterberg, K.L., Boutagy, N.E., McMillan, R.P., Stevens, J.R., Frisard, M.I., Kavanaugh, J.W., et al., 2015. Probiotic supplementation attenuates increases in body mass and fat mass during a high-fat diet in healthy young adults. *Obesity* 23(12):2364–2370.
- [26] Yadav, H., Lee, J.H., Lloyd, J., Walter, P., Rane, S.G., 2013. Beneficial metabolic effects of a probiotic via butyrate-induced GLP-1 hormone secretion. *Journal of Biological Chemistry* 288(35):25088–25097.
- [27] Ramakrishnan, S.K., Shah, Y.M., 2016. Role of intestinal HIF-2 $\alpha$  in health and disease. *Annual Review of Physiology* 78:301–325.
- [28] Shah, Y.M., Matsubara, T., Ito, S., Yim, S.H., Gonzalez, F.J., 2009. Intestinal hypoxia-inducible transcription factors are essential for iron absorption following iron deficiency. *Cell Metabolism* 9(2):152–164.
- [29] Evers, S.S., Shao, Y., Ramakrishnan, S.K., Shin, J.H., Bozadjieva-Kramer, N., Immler, M., et al., 2022. Gut HIF2 $\alpha$  signaling is increased after VSG, and gut activation of HIF2 $\alpha$  decreases weight, improves glucose, and increases GLP-1 secretion. *Cell Reports* 38(3):110270.
- [30] Wang, Y., Kirpich, I., Liu, Y., Ma, Z., Barve, S., McClain, C.J., et al., 2011. *Lactobacillus rhamnosus* GG treatment potentiates intestinal hypoxia-inducible factor, promotes intestinal integrity and ameliorates alcohol-induced liver injury. *American Journal Of Pathology* 179(6):2866–2875 I.
- [31] Deepak, V., Ramachandran, S., Balahmar, R.M., Pandian, S.R., Sivasubramaniam, S.D., Nellaiah, H., et al., 2016. In vitro evaluation of anticancer properties of exopolysaccharides from *Lactobacillus acidophilus* in colon cancer cell lines. *In Vitro Cellular Developmental Biology. Animal* 52(2):163–173.
- [32] Sandberg, A.S., Önning, G., Engström, N., Scheers, N., 2018. Iron supplements containing *Lactobacillus plantarum* 299v increase ferric iron and up-regulate the ferric reductase DCYTB in human caco-2/HT29 MTX Co-cultures. *Nutrients* 10(12):1949.
- [33] Kozich, J.J., Westcott, S.L., Baxter, N.T., Highlander, S.K., Schloss, P.D., 2013. Development of a dual-index sequencing strategy and curation pipeline for analyzing amplicon sequence data on the MiSeq Illumina sequencing platform. *Applied and Environmental Microbiology* 79(17):5112–5120.
- [34] Caporaso, J.G., Kuczynski, J., Stombaugh, J., Bittinger, K., Bushman, F.D., Costello, E.K., et al., 2010. QIIME allows analysis of high-throughput community sequencing data. *Nature Methods* 7(5):335–336.
- [35] Bokulich, N.A., Subramanian, S., Faith, J.J., Gevers, D., Gordon, J.I., Knight, R., et al., 2013. Quality-filtering vastly improves diversity estimates from Illumina amplicon sequencing. *Nature Methods* 10(1):57–59.
- [36] Chao, A., 1984. Nonparametric estimation of the number of classes in a population. *Scandinavian Journal of Statistics*, 265–270, 1984.
- [37] Shannon, C.E., 1948. A mathematical theory of communication. *Bell System Technical Journal* 27:379–423, 623–656.
- [38] Lozupone, C.A., Hamady, M., Kelley, S.T., Knight, R., 2007. Quantitative and qualitative beta diversity measures lead to different insights into factors that structure microbial communities. *Applied and Environmental Microbiology* 73(5):1576–1585.
- [39] Segata, N., Izard, J., Waldron, L., Gevers, D., Miropolsky, L., Garrett, W.S., et al., 2011. Metagenomic biomarker discovery and explanation. *Genome Biology* 12(6):R60.
- [40] Peck, B.C., Mah, A.T., Pitman, W.A., Ding, S., Lund, P.K., Sethupathy, P., 2017. Functional transcriptomics in diverse intestinal epithelial cell types reveals robust MicroRNA sensitivity in intestinal stem cells to microbial status. *Journal of Biological Chemistry* 292(7):2586–2600.
- [41] Safran, M., Kim, W.Y., O'Connell, F., Flippin, L., Günzler, V., Horner, J.W., et al., 2006. Mouse model for noninvasive imaging of HIF prolyl hydroxylase activity: assessment of an oral agent that stimulates erythropoietin production. *Proceedings of the National Academy of Sciences of the United States of America* 103(1):105–110.
- [42] Alquier, T., Poitout, V., 2018. Considerations and guidelines for mouse metabolic phenotyping in diabetes research. *Diabetologia* 61(3):526–538.
- [43] Nuzzo, A., Czernichow, S., Hertig, A., Ledoux, S., Poghosyan, T., Quilliot, D., et al., 2021. Prevention and treatment of nutritional complications after bariatric surgery. *The Lancet. Gastroenterology and Hepatology* 6(3):238–251.
- [44] Das, N.K., Schwartz, A.J., Barthel, G., Inohara, N., Liu, Q., Sankar, A., et al., 2020. Microbial metabolite signaling is required for systemic iron homeostasis. *Cell Metabolism* 31(1):115–130 e6.
- [45] Ma, X., Hua, J., Li, Z., 2008. Probiotics improve high fat diet-induced hepatic steatosis and insulin resistance by increasing hepatic NKT cells. *Journal of Hepatology* 49(5):821–830.